NASA Technical Memorandum 82832

Tribological Evaluation of Composite Materials Made From a Partially Fluorinated Polyimide

Robert L. Fusaro
Lewis Research Center
Cleveland, Ohio

April 1982

NASA

TRIBOLOGICAL EVALUATION OF COMPOSITE MATERIALS MADE FROM A PARTIALLY FLUORINATED POLYIMIDE

by Robert L. Fusaro

National Aeronautics and Space Administration
Lewis Research Center
Cleveland, Ohio

ABSTRACT

Preliminary tribological studies on a new polyimide formulated from the diamine 2,2-bis [4-(4-aminophenoxy)phenyl] hexafluoropane (4-BDAF) indicates polyimides made from this diamine have excellent potential for high temperature applications. Two different polyimides were formulated from the diamine, and five different composites were formulated using one of the polyimides. Composites were made using 10 weight percent (w/o) graphite fluoride powder, 20 w/o PTFE powder, 30 w/o silver powder, or 50 w/o carbon fibers, both graphitic and nongraphitic types. The powder additions did not improve the tribological properties as much as the carbon fibers, and the graphitic fibers produced better results than did the nongraphitic fibers. Results also indicated that improved high temperature stability and tribological properties may be obtained with a polyimide made from the dianhydride pyromellitic acid (PMDA) rather than the dianhydride benzophenonetetracarboxylic acid (BTDA).

E-1199

SUMMARY

Friction, wear, and sliding surface morphological studies of two new polyimides based upon the diamine, 2,2-bis[4-(4-aminophenoxy)phenyl]-hexafluoropane (4-BDAF) were investigated. The dianhydrides used to make the polyimides were pyromellitic acid (PMDA) and benzophenonetetracarboxylic acid (BTDA). The results indicate the co-polyimide formulated with 50 mole percent of the PMDA dianhydride and 50 mole percent of the BTDA dianhydride is a better tribological material than the polyimide formulated with only the dianhydride BTDA. Another advantage of the PMDA formulated polyimide is that it has a higher temperature stability than the BTDA formulated polyimide. The BTDA polyimide has an end use temperature stability of approximately 300° C, the co-polyimide has an end use temperature of approximately 340° C. A polyimide made from only the PMDA dianhydride (not evaluated) would have an end use temperature of approximately 370° C.

Composites formulated using the BTDA based polyimide with 10 w/o graphite fluoride or 30 w/o silver powder additions demonstrated tribological properties equivalent to the polyimide alone. PTFE (20 w/o) powdered weight additions gave improved tribological properties, but were not as good as 50 w/o additions of carbon fibers. Graphitic carbon fibers were found to be superior nongraphitic fibers. The degree of graphitization may be important because one type of graphite fiber evaluated in a previous study produced thick transfer films after long sliding durations which increased adhesion, and thus friction and wear. The graphite fiber used in this study produced thin flowing "layer-like" transfer films which did not build-up. The nongraphitic carbon fiber did not produce this type of transfer film.

The polyimide tended to debond from the fibers, especially at elevated temperatures, indicating improved sizing of the fibers may be necessary. Friction and wear properties of the fiber reinforced polyimide composites tended to increase as temperature increased, but there is some evidence that this may have been accentuated by oxidation of the 440C HT stainless steel counterface at these temperatures.

The fiber reinforced polyimide composites were formulated using 50 weight percent additions of graphite fibers to 50 weight percent additions of polyimide solids. Since the fibers had different densities, the volume ratios are different. Thus, the fiber area in sliding contact is different for each fiber reinforced composite. This may be a reason for the differences observed in tribological properties.

INTRODUCTION

Carbon or graphite fiber reinforced polyimides offer considerable potential for self-lubrication applications where parts are in sliding contact, especially at elevated temperatures. In the aerospace industry, potential uses include liners for self-aligning plain spherical bearings, cages and races for ball and roller bearings, and as a seal material for sliding contact seals. Carbon or graphite fibers improve the strength and stiffness of the composite while also providing lubrication. Polyimide provides the matrix material for holding the fibers, and under certain conditions (such as elevated temperatures (ref. 1)) can improve the friction and wear properties of the composite. Polyimide is also one of the most thermally stable classes of polymers available.

Much research has been conducted on carbon and graphite fiber reinforced polyimides (refs. 2 to 18), and very good friction and wear properties have been found up to 300° C. But higher temperatures are desirable. The factor limiting elevated temperature use of this composite is the thermal stability of the polyimide (ref. 19).

Polyimide is a generic designation and refers to a class of long-chain polymers which have repeated imide groups in the main chain. By varying the monomeric starting materials, polyimides of different chemical composition and structure can be formulated. Each different polyimide possesses its own physical and chemical properties such as: different elastic modulus, different thermal stability, and different glass transition temperatures (T_G). For high temperature applications, the polyimide selected should have the best tribological and physical properties at the elevated end use temperatures.

In 1975, under NASA-Lewis Research Center Contract NAS3-17824, a polyimide was formulated from partially fluorinated polyimide resins prepared from the diamine 2,2-bis[4-(4-aminophenoxy)phenyl] hexafluoropropane (4-BDAF). It possessed great potential for long term service in highly oxidative environments up to 370° C (refs. 20, 21). Because of the promise shown in preliminary physical properties testing, two formulations using this diamine were

used to mold polyimide into pins for friction and wear evaluation. One polyimide was prepared using benzophenonetetracarboxilic acid (BTDA) as the dianhydride, and is designated as 4-BDAF/BTDA. The other polyimide was a copolyimide which consisted of 50 percent (by mole) of the previous polyimide and 50 percent of a polyimide prepared using promellitic acid (PMDA) as the dianhydride, and is designated as 4-BDAF/50BTDA:50PMDA.

Pins were also made using the 4-BDAF/BTDA polyimide and various weight percentages of powdered solid additives or carbon fiber additives. The following composite pins were made: 10 percent graphite fluoride ($(CF_{1.1})_x$), 20 percent PTFE, 30 percent silver, 50 percent graphite carbon fibers, or 50 percent nongraphitic carbon fibers.

The pins were slid against polished 440C HT (high temperature) stainless steel disks under a load of 9.8 N, at temperatures of 25°, 100°, 200°, or 300° C in a 50 percent R. H. controlled air atmosphere at speeds of 0.27 or 2.7 m/s. The results were compared to previous results on graphite fiber reinforced polyimide composites which demonstrated excellent friction and wear results both in pin-on-disk testing (refs. 16 and 18) and in plain spherical bearing testing (refs. 12 to 15).

MATERIALS

Two polyimides based upon a novel aromatic diamine developed under NASA Lewis Contract NAS3-17824 were evaluated. The diamine is shown in figure 1, and is designated 2,2-bis[4-(4-aminophenoxy)pheny] hexafluoropropane or 4-BDAF. One polyimide was prepared using benzophenonetetracarboxilic acid (BTDA) as the dianhydride, and is designated as 4-BDAF/BTDA. The other polyimide evaluated was a copolyimide which consisted of 50 percent (by mole) of the previous polyimide and 50 percent of a polyimide prepared using promellitic acid (PMDA) as the dianhydride, and is designated as 4-BDAF/50BTDA:50PMDA. The preparation of the BDAF and the polyimides made from it is described in references 20 and 21.

In addition to the above two polyimide materials, five composites were formulated using the 4-BDAF/BTDA polyimide as the matrix material. The additives used were 10 weight percent graphite fluoride powder, 20 weight percent polytetrafluoroethylene (PTFE) powder, 30 weight percent silver powder, 50 weight percent of a high modulus graphitic carbon fiber (designated type "HG"), and 50 weight percent of a high modulus nongraphitic carbon fiber (designated type "HC"). Properties or characteristics of the fibers are listed in table I. These composites were compared to a composite which was previously evaluated (refs. 16 and 18) and which was made from a commerically available polyimide (P 13-N) and low modulus graphitic carbon fibers (designated as fiber type "LG"). Properties of these fibers are also given in table I.

The polyimide or the polyimide composite was molded into pins 2.0 cm long and 0.95 cm in diameter. A 0.476 cm radius hemisphere was machined on one end. The hemispherically tipped end was slid against a AISI 440C HT (high temperature) stainless steel disk hardened to Rockwell C-60. The disks were lapped and polished to a centerline average (cla) surface finish of 10^{-7} meter (4 min). Cleaning with levigated alumina did not change this value.

APPARATUS

The pin-on-disk type of friction and wear apparatus used in this study (fig. 2) uses a stationary (0.476 cm radius) hemispherically tipped pin in sliding contact with a flat (6.3 cm diam) 440C HT stainless steel disk. The apparatus was equipped with a variable-speed motor and gear reduction system so that rotational speed could be controlled. The pin slid on a 5.2 cm diameter circular track on the disk. The disk was heated by a high-frequency induction coil. The temperature of the disk was measured by a thermocouple when the disk was not rotating and by an infrared pyrometer when it was in motion. The friction specimens were enclosed in chamber in order to control the atmosphere at 10 000 ppm H_2O (50 percent R.H. at 25° C).

PROCEDURE

Specimen Cleaning

The AISI 440C HT stainless steel disks were cleaned by washing with ethyl alcohol and then by scrubbing with a water paste of levigated alumina. They were then scrubbed with a brush under running distilled water to remove the levigated alumina, and dried with clean compressed air.

The polyimide or polyimide composite pins were scrubbed with a nonabrasive detergent, rinsed with distilled water and dried with clean compressed air.

Experimental Testing

The pin and disk specimens were inserted into the test apparatus and the chamber was then sealed. A controlled moist air test atmosphere (10 000 ppm H_2O) was purged through the chamber for 15 minutes before each test and continuously throughout the test. After purging, the disk was rotated at either 100 or 1000 rpm. Test temperatures of 25, 100, 200, and 300° C were used in this study. The disk was slowly heated to the desired temperature using induction heating and held for 10 minutes at temperature to allow the temperature to stabilize. The load (a 9.8 N weight) was then gradually applied.

At various intervals during the experiments, the tests were stopped and the specimens removed. They were examined by optical microscopy and the wear volume was determined by measuring the wear scar on the hemispherically tipped pin and calculating the volume of material worn away. The pin was not removed from the holder and locating pins insured that it was returned to its original position when it was put back into the apparatus.

RESULTS AND DISCUSSION

Friction and Coefficient

Friction coefficient as a function of sliding distance for the two different polyimides is plotted in figure 3. The temperature was 25° C and the sliding speed was 0.27 m/s (100 rpm). Initially (for about 60 m of sliding), the 4-BDAF/50 BTDA:50PMDA polyimide gave a lower friction coefficient than the 4-BDAF/BTDA polyimide, but for most of the 1 km test it gave higher friction.

The friction coefficient as a function of sliding distance for the three 4-BDAF/BTDA polyimide composites with powder additives is plotted in figure 4. The PTFE additions improved the friction characteristics during the initial stages of sliding, but as sliding continued, the friction coefficient gradually increased to that of the polyimide alone (after 0.7 km of sliding). Graphite fluoride reduced the friction coefficient somewhat but only after 400 meters of sliding. Silver additions slightly increased the friction coefficient of the base 4-BDAF/BTDA polyimide.

Figure 5 presents the friction coefficient as a function of sliding distance for the two carbon fiber reinforced 4-BDAF/BTDA polyimides. Also shown for comparison is a graphite fiber reinforced polyimide composite material which was evaluated previously (refs. 16 and 18) but under different conditions. This composite was made with an additive polyimide (P 13-N) and a low modulus graphite fiber (type "LG"). The P 13-N polyimide composite with the type "LG" fibers gave the lowest friction coefficient after run-in. The 4-BDAF/BTDA composite with the nongraphitic carbon fibers (type "HC") gave a lower friction coefficient than the same polyimide with the graphitic type "HG" fibers for the first 400 meters of sliding, but from 400 to 1000 meters the friction coefficients were about the same. A large increase in friction coefficient for the 4-BDAF/BTDA type "HC" fiber composite occcurred between 400 and 500 meters of sliding (fig. 5). It is postulated that the reason for this was that the polyimide covered the fibers and dominated the friction process.

The four polyimide composites with the lowest friction coefficients were evaluated for longer sliding distances (fig. 6). The composite with PTFE and composites with the type "LG" and type "HC" fibers produced coefficients that tended to increase with sliding distance. Only the 4-BDAF/BTDA polyimide with the type "HG" fiber gave a friction coefficient that remained constant with sliding distance, even up to 100 km of sliding.

To determine if sliding speed had an effect on friction coefficient, the three fiber reinforced polyimides were evaluated at a sliding speed of 2.7 m/s (1000 rpm). The results (fig. 7) indicate that the inital friction coefficients are lower at these higher sliding speeds. The composite with the type "HG" fibers once again had a friction coefficient that remained constant with sliding distance. Possible reasons for this effect will be discussed later in the paper. A comparison of the friction coefficients after 1 kilometer of sliding at 25° C at both 0.27 and 2.7 m/s is shown in figure 8.

The best polyimide composite (4-BDAF/BTDA with type "HG" fibers) was evaluated at the elevated temperatues of 100°, 200°, and 300° C. The sliding speed was 2.7 m/s. The friction coefficient obtained as a function of sliding distance remained relatively constant at these temperatures . Figure 9 compares the friction coefficients obtained after 1 kilometer of sliding for the test temperatures of 25°, 100°, 200°, and 300° C. Also shown are friction coefficients from reference 18 for the P 13-N polyimide reinforced with type "LG" fibers. The friction coefficient for both polyimide composites tended to increase with increasing temperature, although the 4-BDAF/BTDA composite showed a decrease in friction at 300° C. The P 13-N composite tended to produce lower friction coefficients at this sliding distance than did the 4-BDAF/BTDA composites at all temperatures except at 300° C.

Composite Wear Rates

Composite pin wear rates at ambient temperature (23° to 27° C) and a sliding speed of 0.27 m/s are given in table II. Wear rates are presented for selected sliding intervals in an attempt to separate run-in wear from steady state wear and to determine if repeated passes over a surface affected wear rates.

The two unfilled polyimides and the 4-BDAF/BTDA polyimide with silver and graphite fluoride additions did not appear to "run-in". Essentially the same wear rates were obtained for short sliding distances as for longer sliding distances. Wear rate values for these four materials were very high with considerable scatter. The silver and graphite fluoride additions did not reduce wear. Possible reasons for this will be discussed in a later section.

The 4-BDAF/BTDA polyimide with the PTFE additions ran in in less than 0.02 km and the steady state wear rate was an order of magnitude less than the unfilled polyimide. The wear rate had a tendency to decrease with sliding duration and then gradually increase (after 1 km of sliding).

Type "HG" fiber reinforced 4-BDAF/BTDA polyimide and type "LG" fiber reinforced P 13-N polyimide composites produced lower "run-in" wear rates (table II); but it was hard to separate "run-in" from steady wear rates for these composites, since the wear rates continued to gradually decrease with sliding distance after a large inital decrease which occurred before 0.02 km of sliding. The 4-BDAF/BTDA polyimide reinforced with type "HC" fibers also reduced the "run-in" wear rates (table II), but after obtaining a minimum at 0.3 km of sliding, the wear rate gradually increased with sliding duration.

The three fiber reinforced polyimide composites were also evaluated at a sliding speed of 2.7 m/s (1000 rpm), all other conditions being kept constant. The wear rates for a sliding interval of 0 to 1 kilometer for these experiments are lower than those of a sliding speed of 0.27 m/s, but the relative ranking is approximately the same. Figure 10 compares the wear rates from 0 to 1 kilometer of sliding at 25° C and at sliding speeds of 0.27 m/s and 2.7 m/s for all the polyimide composite materials evaluated. Although the composites were formulated using the 4-BDAF/BTDA polyimide as the matrix material, the wear rates (table II and fig. 10) indicate that the other polyimide (4-BDAF/50BTDA:50PMDA) may be a better choice for the matrix material since it produced lower wear rates in the unfilled condition.

The 4-BDAF/BTDA polyimide with type "HG" fibers and the P 13-N polyimide with the type "LG" fibers (ref. 18) were also evaluated at temperatures of 100°, 200°, and 300° C. The wear rates of these composites are compared for a sliding interval of from 0 to 1 kilometer in figure 11. The rate tends to increase exponentially with increasing temperature. Considering experimental error and wear rate repeatability, the wear rates of the two composites can be assumed to be equal. However, at 300° C the wear rate of the composite pin made with the 4-BDAF/BTDA polyimide is about three times higher than the composite pin made with the P 13-N polyimide. A possible reason for this is that the softing point (T_G) of the 4-BDAF/BTDA polyimide is 304° C; and frictional heating may have produced even higher temperatures in the contact

zone. Softing of the polyimide would produce higher wear. The T_G of the P 13-N polyimide is approximately 315° C. This slightly higher T_G seems to have been sufficient to improve the wear properties.

Long duration wear rates of the three fiber reinforced polyimides composites are summarized in table III. For long durations of sliding, both the type "HC" fiber reinforced 4-BDAF/BTDA polyimide and type "LG" fiber reinforced P 13-N polyimide composites produced wear rates that tended to increase with sliding duration. For the type "HG" fiber reinforced 4-BDAF/BTDA polyimide composite, the wear rate tended to decrease or remain constant with sliding duration, especially at 25° and 100° C.

Wear Surface Morphology

Unfilled polyimides. - Photomicrographs of the 4-BDAF/BTDA polyimide rider surface after 200 meter of sliding at 100 rpm and 25° C are shown in figure 12. In general, the surface is very smooth, but there are areas where voids exist. Most likely these were produced during the molding process rather than during the wear process. Very fine powdery wear could be seen on the scar. When viewed between polarizing filters the debris is seen to be birefringent, indicating it is anistropic crystalline.

Photomicrographs of the 4-BDAF/50BTDA:50PMDA polyimide rider surface after 1000 meter of sliding at 100 rpm (0.27 m/s) and 25° C are shown in figure 13. The surface looks similar to the other polyimide, except that striations can be seen in the sliding direction and that the wear debris had a tendency to coalesce together more than with the other polyimide. Powdery, birefringent wear debris was also found, but a lesser amount.

Powder filled polyimides. - Photomicrographs of the 4-BDAF/BTDA polyimide rider surface, which was filled with 10 weight percent graphite fluoride ($(CF_{1.1})_x$), after 20 meter of sliding at 100 rpm and 25° C is shown in figure 14. The surface has more voids than was found for the unfilled polyimide and a much larger quantity of powdery, birefringent wear debris. What appears to have happened is that the graphite fluoride did not evenly disperse throughout the polyimide matrix and instead clustered together in small pockets throughout the polyimide. As wear occurred, the graphite fluoride was released from the pocket leaving a void. The graphite fluoride released in this manner did not reduce friction and wear.

A photomicrograph of the 4-BDAF/BTDA polyimide surface filled with 30 weight percent silver powder is shown in figure 15 after 20 meter of sliding at 100 rpm and 25° C. The silver particles can readily be seen in the wear scar, but their presence provided no lubrication benefits. They had a tendency to spall and leave a void and did not appear to strengthen the polyimide matrix.

Photomicrographs of the 4-BDAF/BTDA polyimide rider surface with 20 weight percent PTFE powder additions is shown in figure 16 after 10 kilometer of sliding at 100 rpm (.27 m/s) and 25° C. Like graphite fluoride, the PTFE did

not appear to be evenly dispersed. This was true especially during the early stages of sliding where very irregular shaped wear scars were produced. Figure 16 shows PTFE agglomeration, spalls and transverse cracks.

Fiber reinforced polyimides. - Figure 17 shows photomicrographs of the 4-BDAF/BTDA polyimide rider wear surface, which was reinforced with type "HC" fibers, after 4 kilometers of sliding at 100 rpm and 25° C. The wear surface indicates that the fibers were not evenly dispersed and that they tended to cluster together. The polyimide also tended to spall from the fibers, which indicated that the bond between the fiber and polyimide was poor. The fibers, and the polyimide surface which did not spall, possessed a very smooth surface finish.

Figure 18 shows photomicrographs of the 4-BDAF/BTDA polyimide rider reinforced with the type "HG" fibers after 3 kilometer of sliding at 100 rpm and 25° C. Uneven dispersal and clustering of the fibers was again observed, but the polyimide appears to be bonded to the type "HG" fibers more tightly than to the type "HC" fibers. Spalls were observed which involved both the fibers and polyimide. Back transfer from the disk occurred, with the transferred material adhering predominately to the fibers.

Figure 19 presents photomicrographs of the P 13-N polyimide rider reinforced with the type "LG" fibers after (a) 0.5 km and (b) 10 km of sliding at 100 rpm and 25° C. The composites were produced by the same vendor and had the same 1 to 1 ratio by weight of polyimide solids and graphite or carbon fiber solids. Comparison of the wear surfaces in figures 17 to 19 indicate that the P 13-N had a much greater surface density of graphite fibers. The reason is that the type "LG" fibers had a lower specific gravity than the type "HG" or type "HC" fibers (table I).

Also seen in the figures is the un-even dispersal and clustering of the fibers. Very little spalling is seen, and that which did occur was due to debonding of fibers parallel to the sliding surface (fig. 19(b)). Some imbedded wear debris was observed in the polyimide matrix material.

Transfer Films at 25° C

Unfilled polyimides. - Photomicrographs of typical transfer films on 440C HT stainless steel disks from (a) 4-BDAF/BTDA and (b) 4-BDAF/50BTDA:50PMDA are shown in figure 20. The transfer characteristics of both polyimides appear very similar. Flat platelet-like particles tend to fill the low spots or valleys on the metallic surface. If any difference does exist, it appears that the 4-BDAF/50BTDA:50PMDA polyimide has slightly better plastic flow properties than the 4-BDAF/BTDA polyimide (fig. 20).

Powder filled polyimides. - Transfer from the 4-BDAF/BTDA polyimide filled with 10 weight percent graphite fluoride or 30 weight percent silver powder exhibited transfer very similar to the unfilled polyimide. Twenty weight percent additions of PTFE powder to the polyimide initiated the production of very thin plastically flowing transfer films. Figure 21 shows typical transfer to the same region on the metallic disk after (a) 1 kilometer and (b) 4 kilometer of sliding at 25° and 100 rpm. The figure illustrates that the transferred material is in constant motion and that its thickness tends to increase with sliding duration.

Fiber reinforced polyimides. - Photomicrographs of the transfer to a 440C HT stainless steel disk from the 4-BDAF/BTDA polyimide reinforced with type "HC" fibers is shown in figure 22 for sliding intervals of 1, 2, and 4 kilometers of sliding at 100 rpm and 25° C. These transfer films are typical also of those at 1000 rpm. The transfer tends to fill low areas (scratches, indentations, etc.), but does not produce plastically flowing films on the higher regions.

Figure 23 shows transfer to 440C HT stainless steel disks from the 4-BDAF/BTDA polyimide reinforced with type "HG" fibers after 1, 10 and 60 kilometers of sliding at 25° C and 100 rpm. Similar transfer occurred at 1000 rpm. Thin plastically flowing transfer occurred that covered the entire wear track surface. The thickness of the transfer was in the order of the wavelength of light (0.4 to 0.8 micrometers), and the transfer remained approximately this thickness for the duration of the test (100 km).

P 13-N polyimides reinforced with type "LG" fibers also demonstrated this type of transfer for short sliding distances. But as sliding distance increased, transfer increased to "local" thickness values of greater than 10 micrometers. In reference 18 it was postulated that this increase in thickness was responsible for increases in adhesion between the surfaces, thus increases in friction and wear.

Morphology and Transfer at Elevated Temperatures

Photomicrographs of the 4-BDAF/BTDA polyimide rider wear surfaces which were reinforced with type "HG" fibers are shown in figure 24 after 1 kilometer of sliding at temperatures of 100, 200, and 300° C. The polyimide tended to debond from the fibers at a faster rate as temperature increased. As seen in figure 24, the fibers appear to be relatively uneffected by temperature, and at 300° C (fig. 24(c)) only the fibers appear to be supporting the load. At 100° C considerably more backtransfer occurs than at 25° C, and the surface shows a mixing of constituents (fig. 24(a)). The P 13-N polyimide composites reinforced with type "LG" fibers showed similar characteristics as the temperature was increased, except that at 100° C there was less backtransfer and mixing together of constituents (ref. 18).

Photomicrographs of the transfer to 440C stainless steel disks from the type "HG" fiber reinforced 4-BDAF/BTDA composite after 1 kilometer of sliding at 100, 200, or 300° C is shown in figure 25. The transfer is more continuous than was found for the 25° C test (fig. 23), but it is not as thick. As temperature increased the transfer tended to fill only the low spots on the metallic surface; and as the polyimide was depleted (fig. 24), the fibers tended to have a polishing effect on the high areas in the wear track (fig. 25), with little transfer occurring. The wear track also tended to take on a reddish appearance at elevated temperatures, which indicates that oxidation of the metal may have occurred. This aspect warrants further investigation.

Geometry Considerations

The composite specimens in this study were evaluated as hemispherically tipped pins sliding against 440C HT stainless steel counterfaces. This

geometry was chosen since it closely approximates the geometry of a sliding contact seal, which is a possible end use application of the composite.

It should be indicated that geometry can markedly affect the tribological properties of these composites. For example, in reference 18, the tribological properties of a P 13-N polyimide with type "LG" fibers were compared for the case when the pin was made from the composite and slid against a 440C HT stainless steel disk counterface and for the case when a 440C HT stainless steel pin was slid against a disk made of the composite. In both cases no measureable wear occurred to the metallic specimen, but the friction and wear properties of the composite were completely different. When the pin was made from the composite, friction and composite wear tended to increase with increasing temperature; but when the disk was made of the composite, friction tended to decrease and composite wear was constant with increasing temperature.

These results indicate the importance of carefully choosing the experimental parameters when comparing tribological materials. It also indicates that materials should be evaluated in such a manner that geometry is carefully considered.

CONCLUSIONS

Preliminary friction, wear, and surface morphological studies of two polyimides made by the polymerization of a new diamine (4-BDAF) with two different dianhydrides (BTDA and PMDA) and of five different composites made from one of the polyimides (4-BDAF/BTDA) indicate that:

1. This new diamine shows considerable potential for making polyimides which will exhibit better tribological properties at higher temperatures.

2. Polyimides made from the dianhydride 50 BTDA:50 PMDA exhibited better tribological properties than those made with BTDA alone; indicating that PMDA may be a better dianhydride to use than BTDA.

3. Carbon fiber or graphite fiber additions gave much better tribological properties than powdered additions of PTFE, graphite fluoride, or silver. Graphitic carbon fibers performed better than nongraphitic carbon fibers.

4. The friction coefficients and wear rates of fiber reinforced polyimide composites increase with increasing temperature. This may have been partly due to oxidation of the 440C HT stainless steel counterface.

5. Wear surface morphology of the fiber reinforced polyimides indicated that the polyimide tended to debond from the fiber at elevated temperatures, indicating the need for improved sizing of the fibers.

6. Surface morphology also indicated that the fiber to polyimide surface area on the composite wear scar varied as the density of the fiber varied, indicating the composites should be formulated on a volume rather than a weight basis.

REFERENCES

1. Fusaro, Robert L.: Polyimide Film Wear - Effect of Temperature and Atmosphere. NASA TN D-8231, 1976.

2. Giltrow, J. P. and Lancaster, J. K., "Properties of Carbon-Fibre-Reinforced Polymers Relevant to Applications in Tribology," London, Plastics Institute, International Conference on Carbon Fibres, Their Composites and Applications, February 1971, Paper 31.

3. Giltrow, J. P. and Lancaster, J. D., "Friction and Wear of Polymers Reinforced with Carbon Fibers," Nature 214, 1106-1107 (1967).

4. Lancaster, J. K., "The Effect of Carbon Fibre Reinforcement on the Friction and Wear of Polymers," J. Phys. D. 1, 549-559 (1968).

5. Giltrow, J. P., "A Design Philosophy for Carbon Fibre Reinforced Sliding Components," Tribology 4, (1) 21-28 (1971).

6. Harris, C. L. and Wyn-Roberts, D., "Wear of Carbon Fibre Reinforced Polymers in a High Vacuum Environment," Nature 217, 981-982 (1968).

7. Giltrow, J. P. and Lancaster, J. K., "Carbon-Fibre Reinforced Polymers as Self-Lubricating Materials," Tribology Convention, Pithochry, Scotland, May 15-17, 1968, Proceedings, Institution of Mechanical Engineers, pp. 149-159 (1968).

8. Giltrow, J. P. and Lancaster, J. K., "The Role of the Counterface in the Friction and Wear of Carbon Fibre Reinforced Thermosetting Resins," Wear 16, (11) 359-374 (1970).

9. Simon, R. A. and Prosen, S. P., "Graphite Fiber Composites; Shear Strength and Other Properties," Twenty-Third Annual Technical Conference, SPI Reinforced Plastics Composite Division, Proceedings, Society of the Plastics Industry, Inc., Section 16-B, pp. 1-10 (1968).

10. Herrick, J. W., "Bearing Materials from Graphite Fiber Composites," Reinforced Plastics - Ever New; Proceedings of the Twenty-Eighth Annual Technical Conference, Society of the Plastics Industry, Inc., 17-D, 1-17-D, 6 (1973).

11. Giltrow, J. P., "The Influence of Temperature on the Wear of Carbon Fiber Reinforced Resins," ASLE Trans. 16, (2) 83-90 (1973).

12. Sliney, H. E. and Johnson, R. L., "Graphite Fiber-Polyimide Composites for Sperical Bearings to 340° C (650° F)," NASA TN D-7078 (1972).

13. Sliney, H. E., Jacobson, T. P., and Munson, H. E., "Dynamic Load Capacities of Graphite-Fiber - Polyimide Composites in Oscillating Plain Bearings to 340° C (650° F)," NASA TN D-7880 (1975).

14. Sliney, H. E. and Jacobson, T. P., "Performance of Graphite Fiber-Reinforced Polyimide Composites in Self-Aligning Plain Bearings to 315° C," Lubr. Eng. 31, (12) 609-613 (1975).

15. Sliney, H. E. and Jacobson, T. P., "Some Effects of Composition on Friction and Wear of Graphite-Fiber-Reinforced Polyimide Liners in Plain Spherical Bearings," NASA TP 1229 (1978).

16. Fusaro, R. L. and Sliney, H. E., "Friction and Wear Behavior of Graphite Fiber Reinforced Polyimide Composites," ASLE Trans., 21 (4) 337-343 (1978).

17. Lancaster, J. K., "Geometrical Effects on the Wear of Polymers and Carbons," Lubr. Technol., 97 (2) 187-194 (1975).

18. Fusaro, R. L.: Geometrical Aspects of the Tribological Properties of Graphite Fiber Reinforced Polyimide Composites. NASA TM 82757 (1982).

19. Fusaro, R. L.: Tribological Properties and Thermal Stability of Various Types of Polyimide Films. NASA TM 81765 (1981).

20. Jones, R. J.; O'Rell, M. K.; and Hom, J. M.: Polyimides Prepared from Perfluoroisopropylidene Diamine. U.S. Patent 4,111,906, Sept. 5, 1978.

21. Jones, R. J.; O'Rell, M. K.; and Hom, J. M.: Fluorinated Aromatic Diamine. U.S. Patent 4,203,922, May 20, 1980.

TABLE I. - TYPICAL FIBER PROPERTIES

Property or characteristic	Graphite fiber Type "LG"(a)	Carbon Fiber	
		Type "HC"(b)	Type "HG"(c)
Tensile strength	6.2×10^8 N/m^2	1.6×10^9 N/m^2	1.9×10^9 N/m^2
Elastic modulus	3.0×10^{10} N/m^2	2.6×10^{11} N/m^2	5.2×10^{11} N/m^2
Length	6×10^{-3} m	6×10^{-3} m	6×10^{-3} m
Diameter	8×10^{-6} m	8×10^{-6} m	6×10^{-6} m
Specific gravity	1.4	1.75	1.96
Graphitic	YES	NO	YES
Carbon assay	99.5 percent	99 percent	99.9 percent

(a) Low modulus, graphitic
(b) High modulus, nongraphitic
(c) High modulus, graphitic

TABLE II. - WEAR RATES OF SEVERAL COMPOSITE TYPES FOR VARIOUS INTERVALS OF SLIDING AT 25° C AND 100 rpm

Composite type	Wear rate $m^3/mx10^{-15}$											
	Sliding interval, km											
	0→.02	.02→.05	.05→.10	.10→.20	.20→.30	.30→.50	.5→1.0	1.0→2.0	2.0→4.0	4.0→10	10→20	20→100
BTDA unfilled	240	190	65	110	130	130	230	-	-	-	-	-
BTDA/PMDA	21	19	62	89	41	41	23	-	-	-	-	-
BTDA/silver	330	190	150	87	130	110	160	-	-	-	-	-
BTDA/CF_x	430	30	150	200	150	130	140	-	-	-	-	-
BTDA/PTFE	130	12	17	15	6	9	3	7	11	15	-	-
BTDA/Type "HC" fiber	51	6	2	4	1	3	5	6	8	20	-	-
BTDA/Type "HG" fiber	52	13	11	5	6	3	3	2	2	2	1	1
BTDA/Type "LG" fiber	21	14	6	6	3	3	2	2	1	1	-	-

TABLE III. - LONG DURATION WEAR RATES OF THREE FIBER REINFORCED POLYIMIDE COMPOSITES FOR SLIDING SPEEDS OF 100 and 1000 rpm AT TEMPERATURES OF 25, 100, 200 and 300° C

Polyimide type	Fiber type	Temp, °C	Speed, rpm	Wear Rate $m^3/mx10^{-15}$						
				Sliding Interval, km						
				0→1	1→2	2→4	4→10	10→20	20→50	50→100
BTDA	"HC"	25° C	100	5	6	8	25	-	-	-
			1000	3	3	6	3	20	-	-
BTDA	"HG"	25° C	100	6	2	2	2	1	2	1
			1000	3	.4	2	3	2	2	1.5
		100° C	1000	11	19	35	-	-	-	-
		200° C	1000	54	-	-	-	-	-	-
		300° C	1000	420	-	-	-	-	-	-
P 13-N	"LG"	25° C	100	4	2	1.5	1	-	-	-
		25° C	1000	3	2	3	4	4	12	-
		100° C	1000	18	24	33	40	-	-	-
		200° C	1000	68	-	-	-	-	-	-
		300° C	1000	195	-	-	-	-	-	-

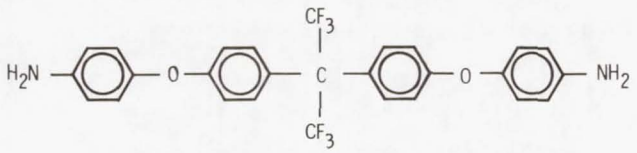

Figure 1. - Aromatic diamine used to formulate polyimides.

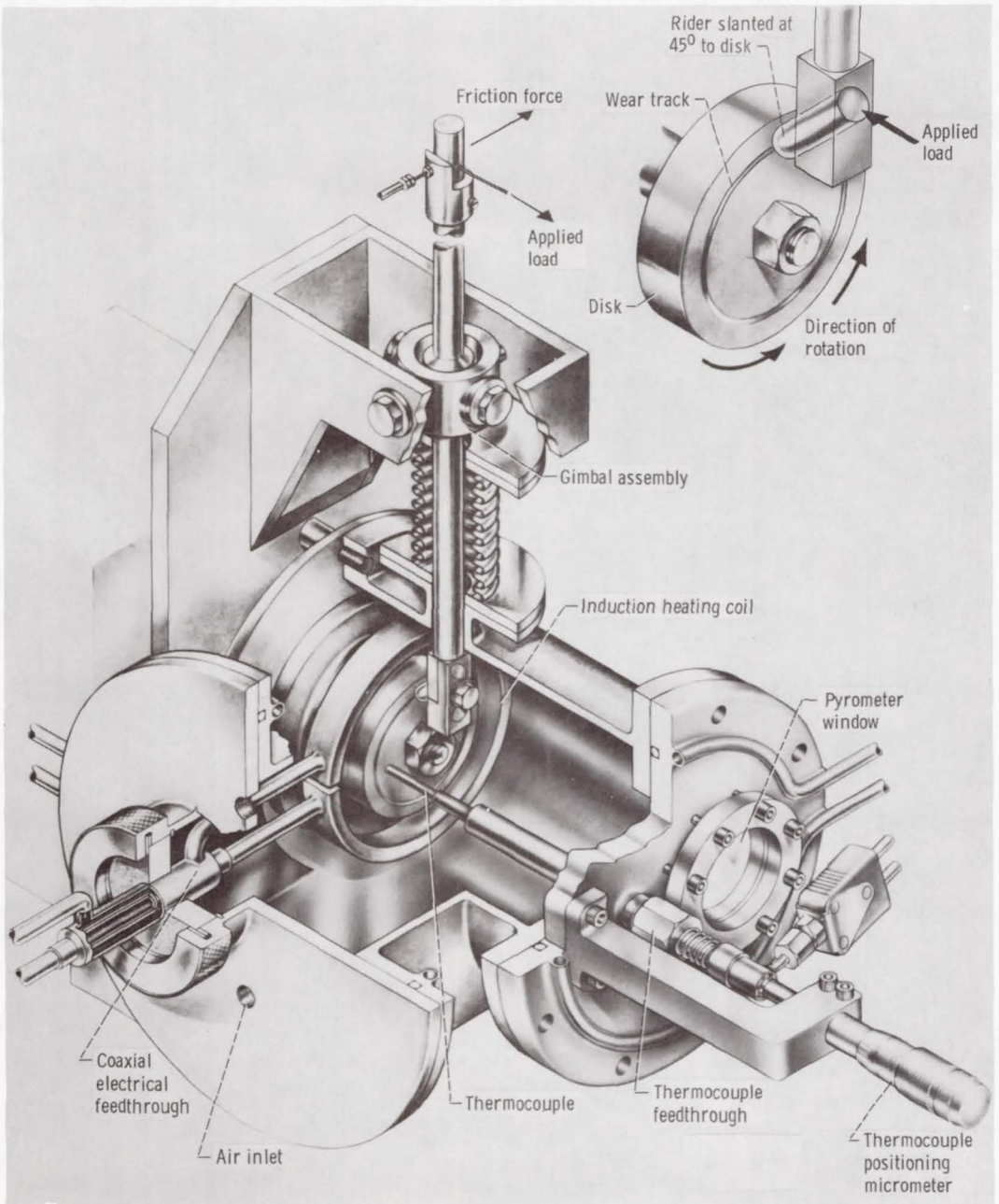

Figure 2. - Friction and wear experimental apparatus. Experimental conditions: atmosphere, 50% R.H. air; load, 9.8 N; disk (counterface) material, 440C HT stainless steel (4 μin. cla); temperatures, 25°, 100°, 200°, or 300° C; sliding speed, 100 rpm (0.27 m/s) or 1000 rpm (2.7 m/s).

CD-12384-26

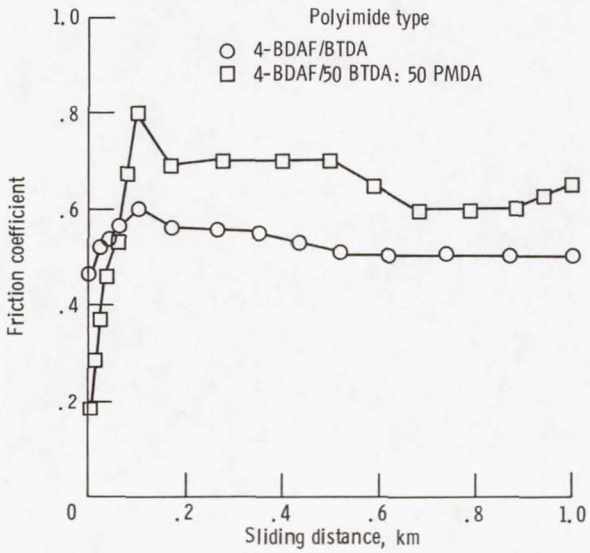

Figure 3. - Friction coefficient as a function of sliding distance for 4-BDAF/BTDA and 4-BDAF/50 BTDA: 50 PMDA unfilled polyimide riders sliding against a 440C HT stainless steel counterface at 25° C and 0.27 m/s (100 rpm).

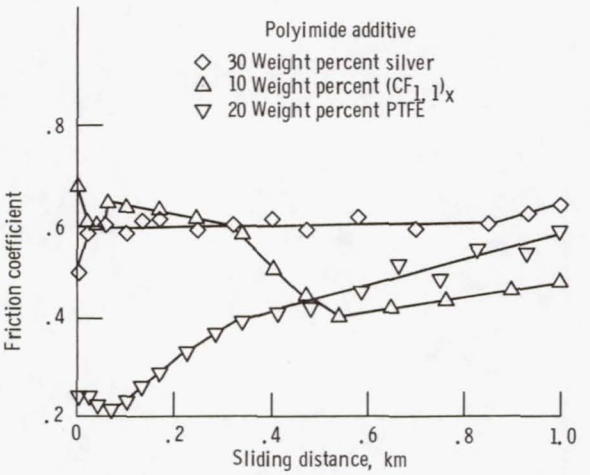

Figure 4. - Friction coefficient as a function of sliding distance for 4-BDAF/BTDA polyimide riders filled with 10 weight percent $(CF_{1.1})_x$, 20 weight percent PTFE or 30 weight percent silver powder sliding against a 440C HT stainless steel counterface at 25° C and 0.27 m/s (100 rpm).

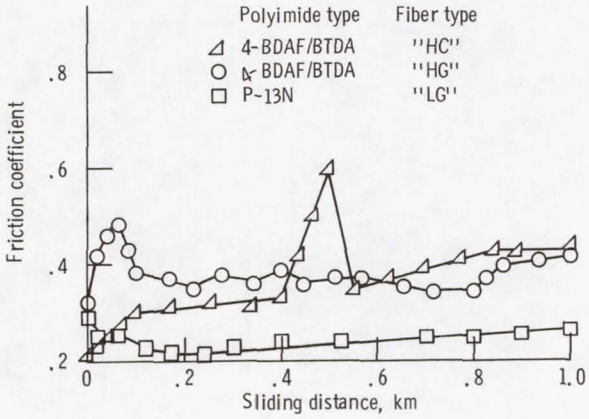

Figure 5. - Friction coefficient as a function of sliding distance for three fiber reinforced polyimide composite riders sliding against a 440C HT stainless steel counterface at 25° C and 0.27 m/s (100 rpm).

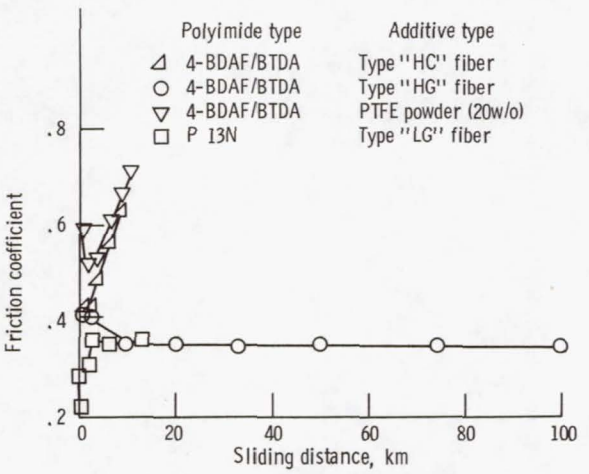

Figure 6. - Friction coefficient as a function of long sliding distances for various polyimide composite riders sliding against a 440C HT stainless steel counterface at 25° C and 0.27 m/s (100 rpm).

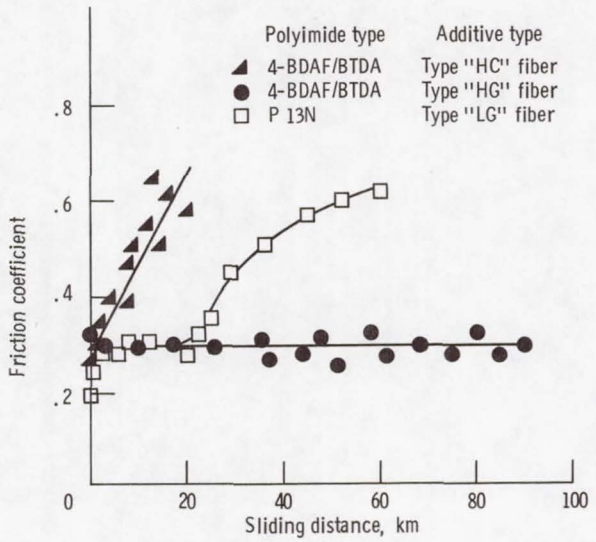

Figure 7. - Friction coefficient as a function of long sliding distances for fiber reinforced polyimide composite riders sliding against a 440C HT stainless steel counterface at 25° C and 2.7 m/s (1000 rpm).

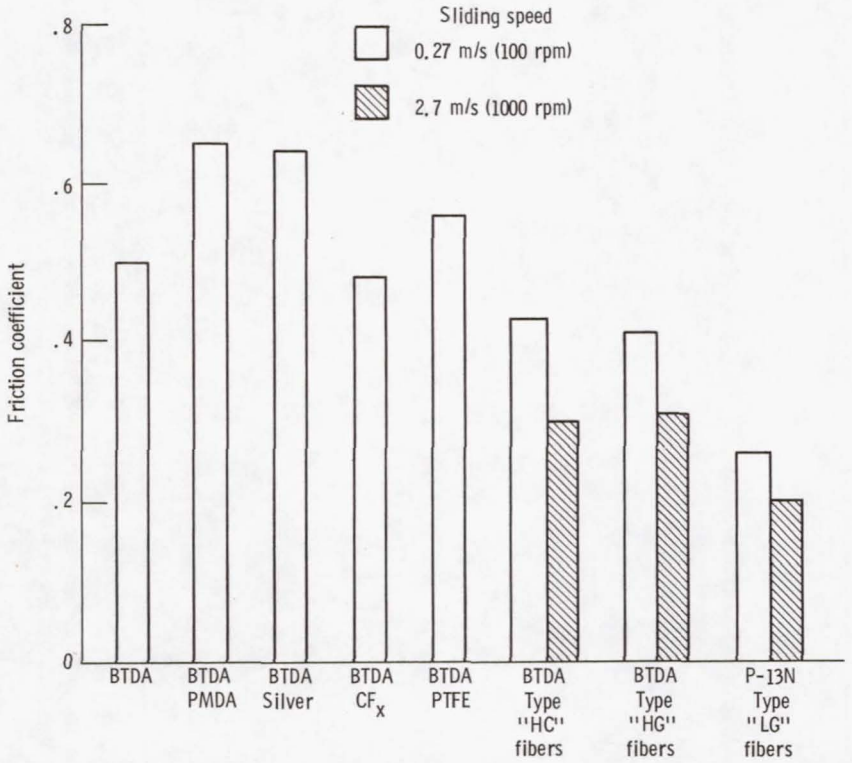

Figure 8. - Comparison of average friction coefficients at 25° C from 0 to 1 kilometer of sliding.

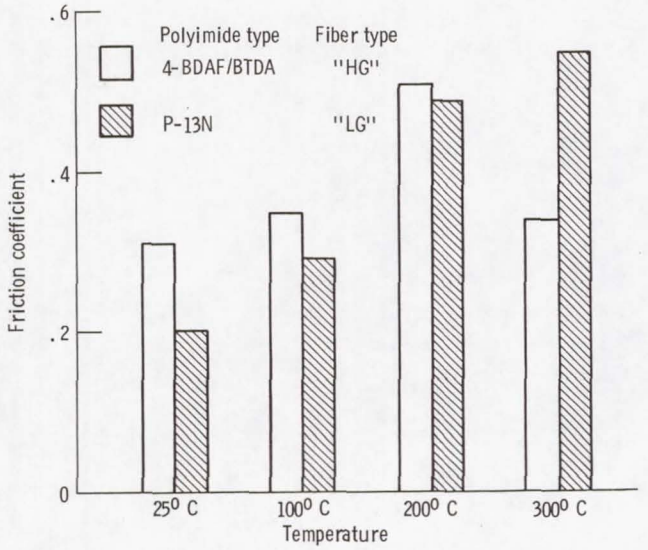

Figure 9. - Effect of temperature on average friction coefficient at 1000 rpm from 0 to 1 kilometer of sliding.

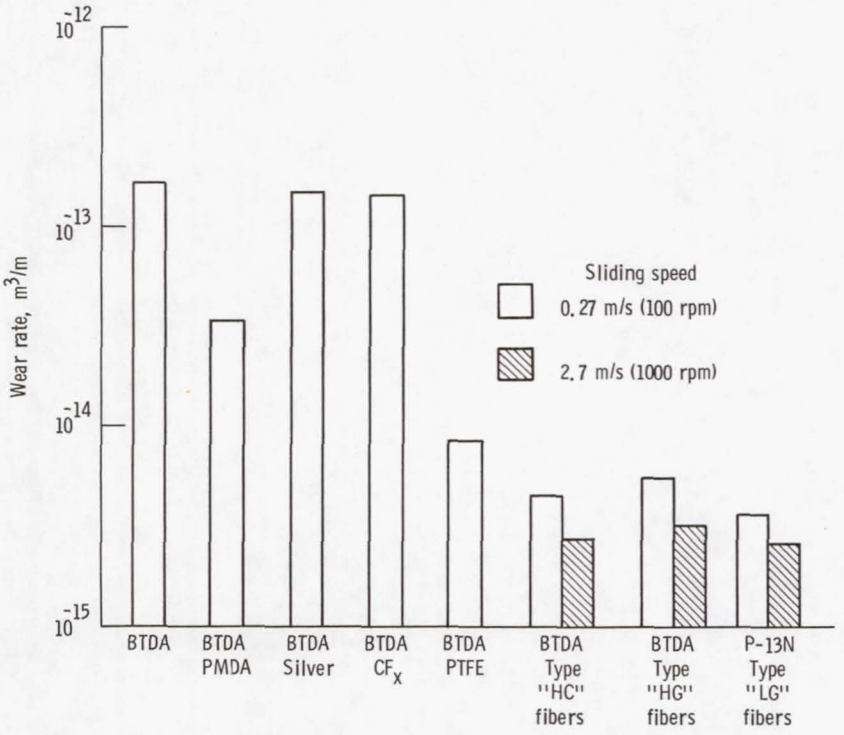

Figure 10. - Comparison of wear rates from 0 to 1 kilometer of sliding at 25° C.

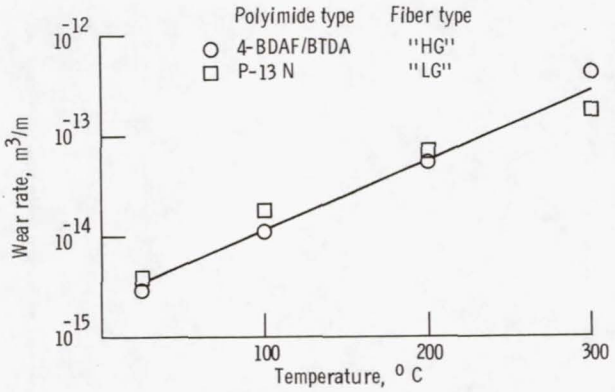

Figure 11. - Effect of temperature on the wear rate of fiber reinforced polyimide composite riders for sliding intervals of 0 to 1 kilometer at 2.7 m/s (1000 rpm).

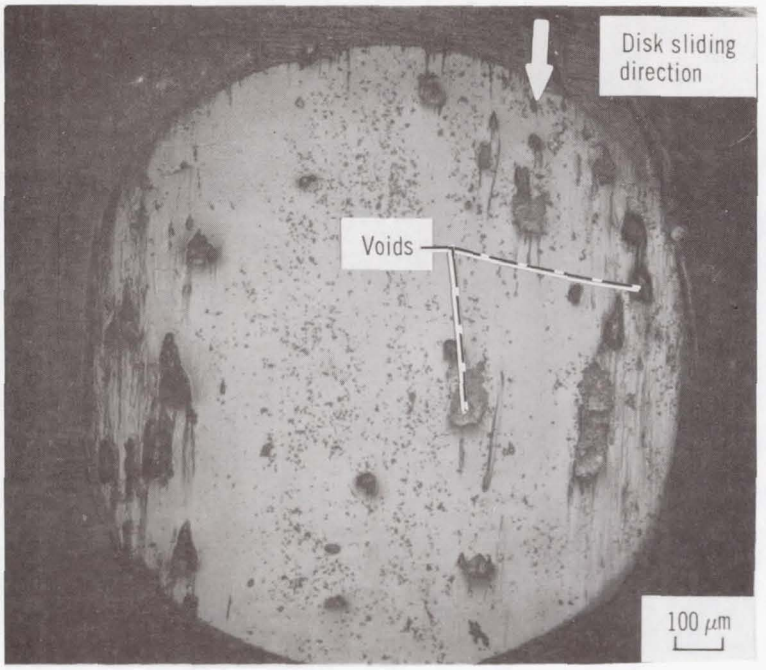

(a) Overview of rider wear scar.

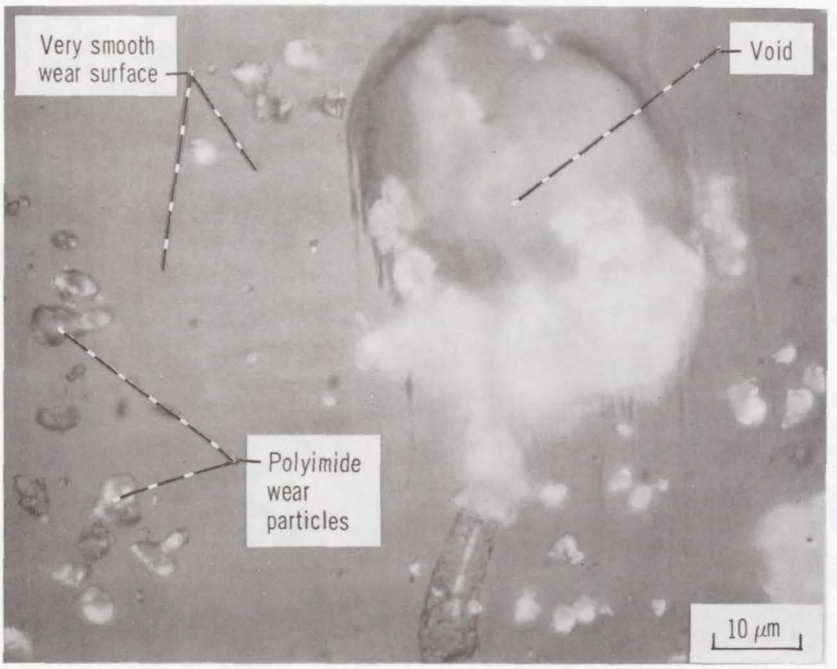

(b) High magnification view of region within the wear scar.

Figure 12. - Photomicrographs of the wear scar on a 4-BDAF/BTDA polyimide rider after 200 meter of sliding at 25° C and 100 rpm.

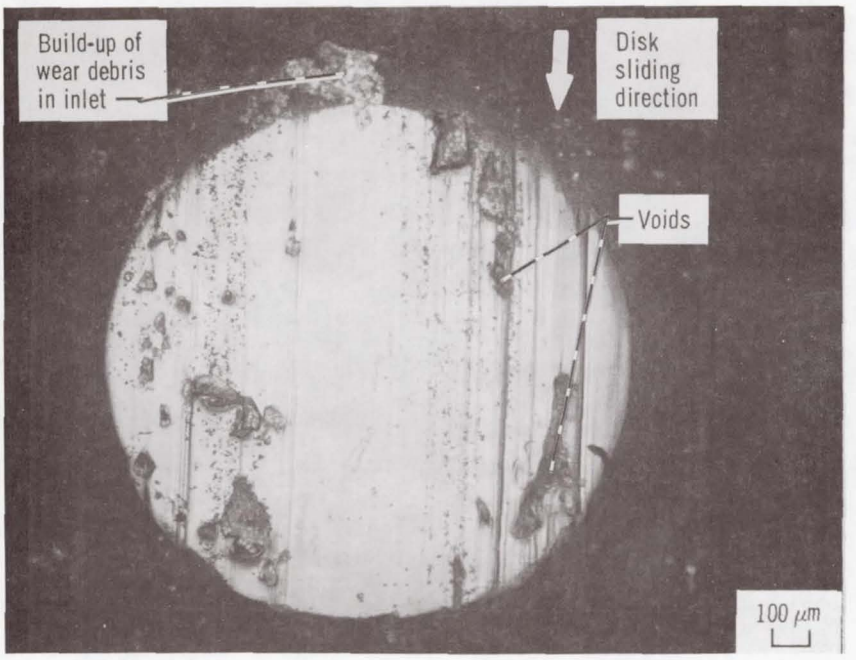

(a) Overview of rider wear scar.

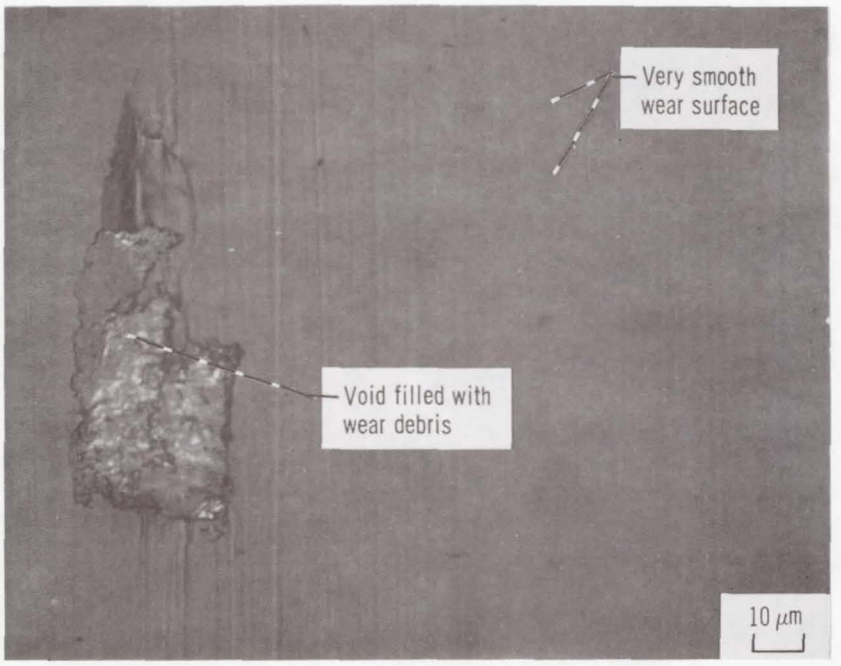

(b) High magnification view of region within the wear scar.

Figure 13. - Photomicrographs of the wear scar on a 4-BDAF/50BTDA:50PMDA polyimide rider after 1 kilometer of sliding at 25° C and 100 rpm.

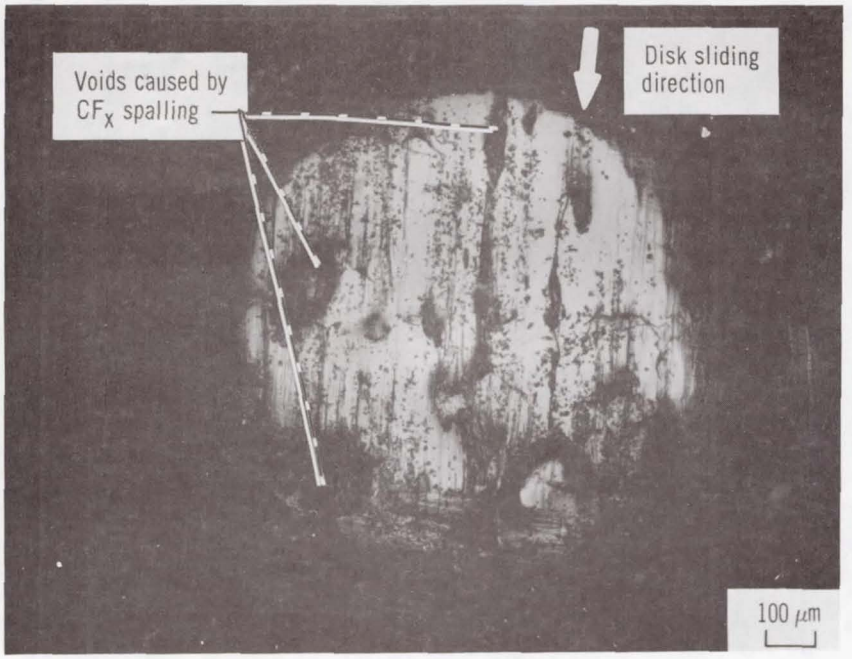

(a) Overview of rider wear scar.

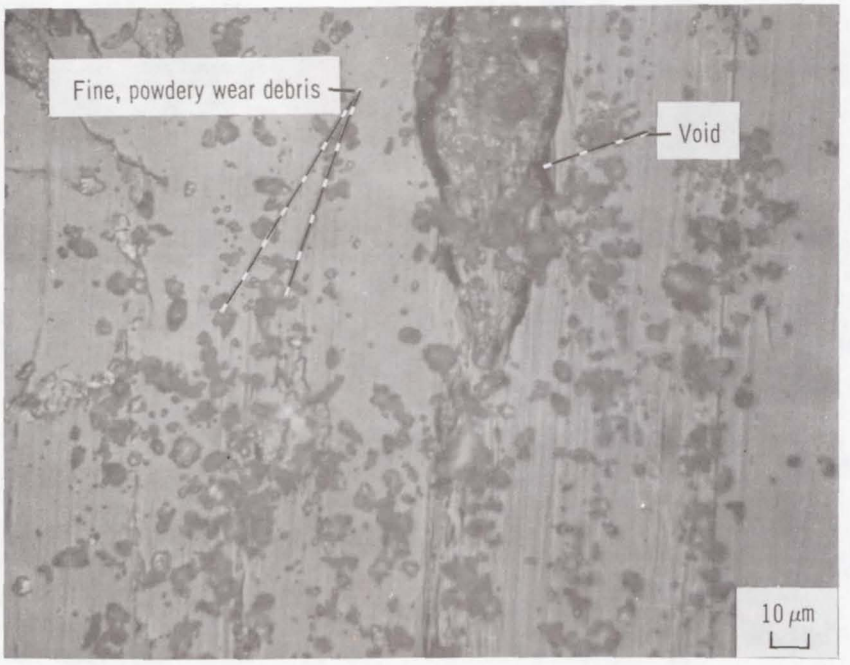

(b) High magnification view of region within wear scar.

Figure 14. - Photomicrographs of the wear scar on a 4-BDAF/BTDA polyimide rider filled with 10 weight percent graphite fluoride ($CF_{1.1}$) powder after 20 meters of sliding at 25° C and 100 rpm.

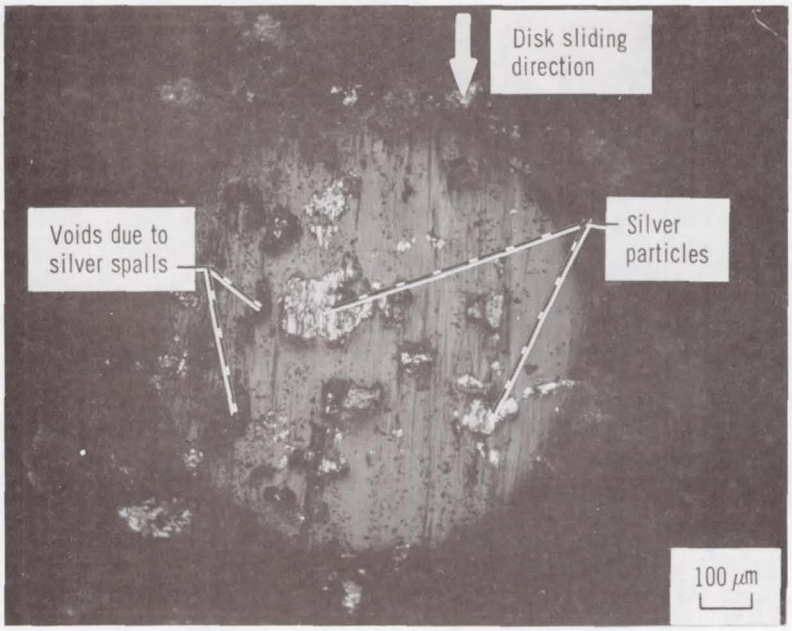

Figure 15. - Photomicrograph of the wear scar on a 4-BDAF/BTDA polyimide rider filled with 30 weight percent silver powder after 20 meters of sliding at 25° C and 100 rpm.

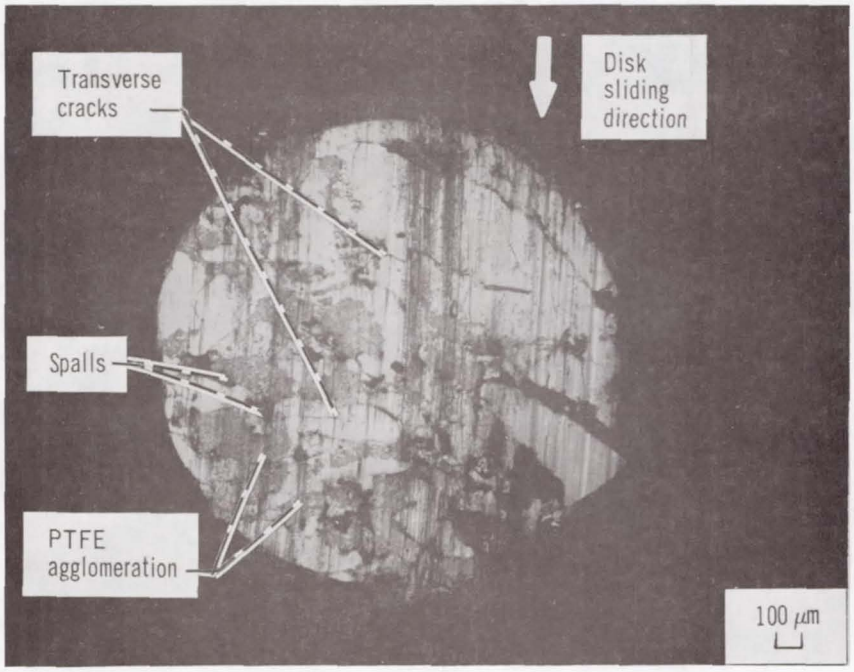

Figure 16. - Photomicrograph of the wear scar on a 4-BDAF/BTDA polyimide rider filled with 20 weight percent PTFE powder after 10 kilometers of sliding at 25° C and 100 rpm.

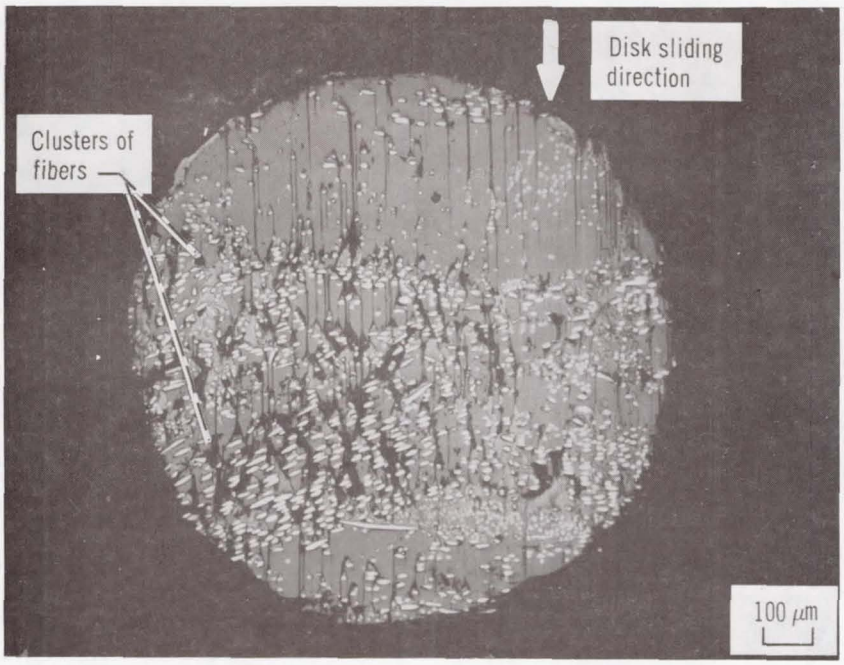

(a) Overview of rider wear scar.

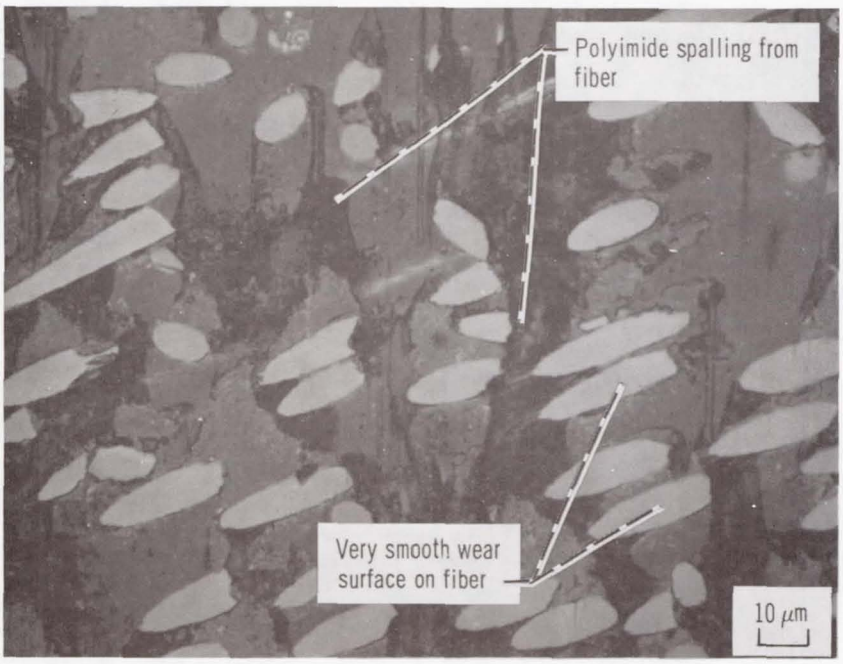

(b) High magnification view of region within wear scar.

Figure 17. - Photomicrographs of the wear scar on a non-graphitic carbon fiber (type "HC") reinforced polyimide (4-BDAF/BTDA) composite after 4 kilometers of sliding at 25° C and 100 rpm.

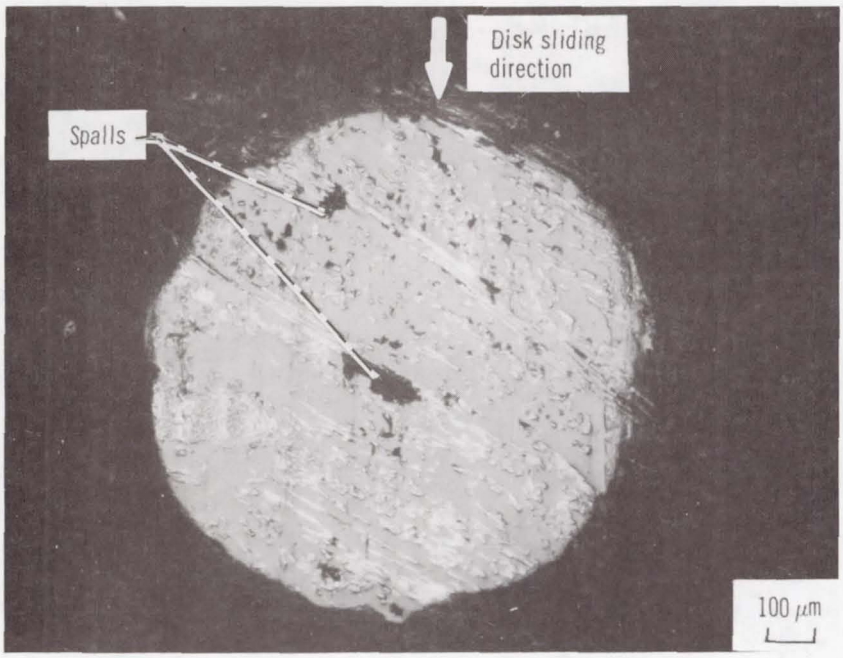

(a) Overview of rider wear scar.

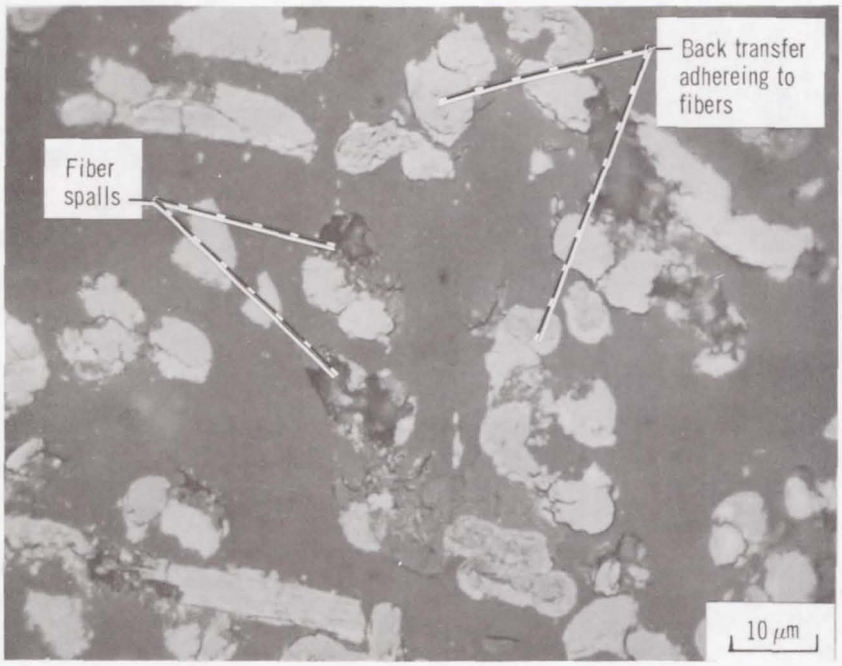

(b) High magnification view of region within wear scar.

Figure 18. - Photomicrographs of the wear scar on a graphitic carbon fiber (type "HG") reinforced polyimide (4-BDAF/BTDA) composite after 3 kilometers of sliding at 25° C and 100 rpm.

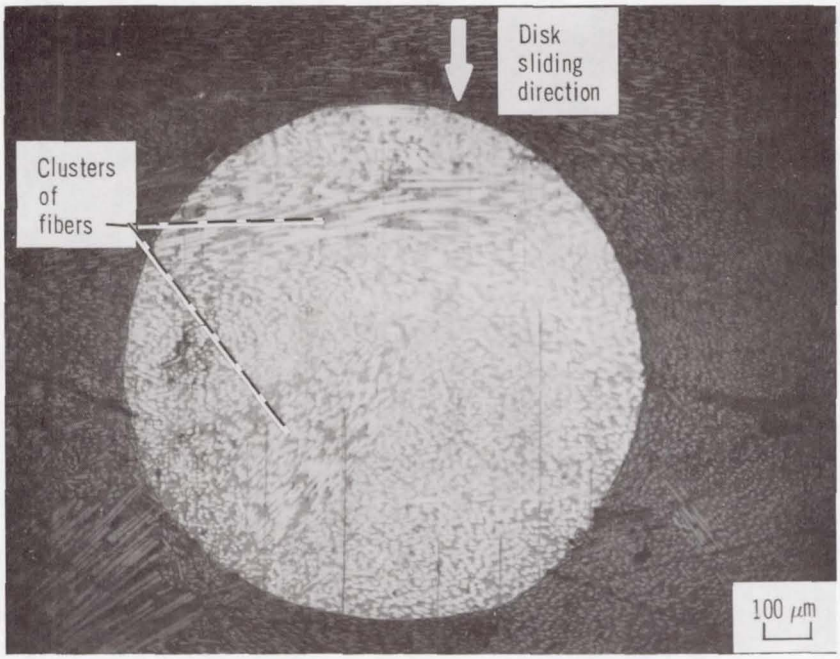

(a) Overview of rider wear scar (0.5 km of sliding).

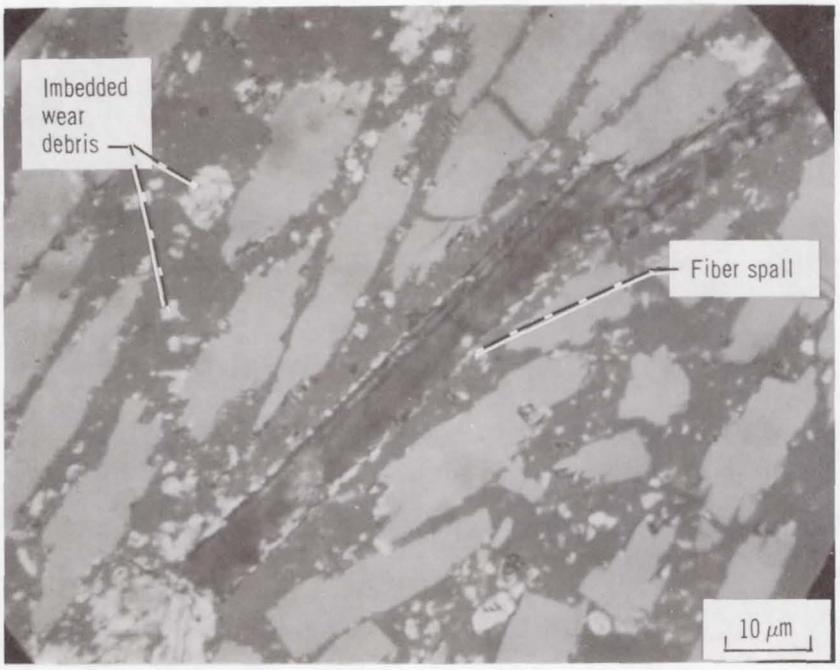

(b) High magnification view of region within wear scar (10 km of sliding).

Figure 19. - Photomicrographs of the wear scar on a low modulus graphite fiber (type "LG") reinforced polyimide (P13-N) composite after various sliding intervals at 25° C and 100 rpm.

(a) Transfer from 4-BDAF/BTDA polyimide rider.

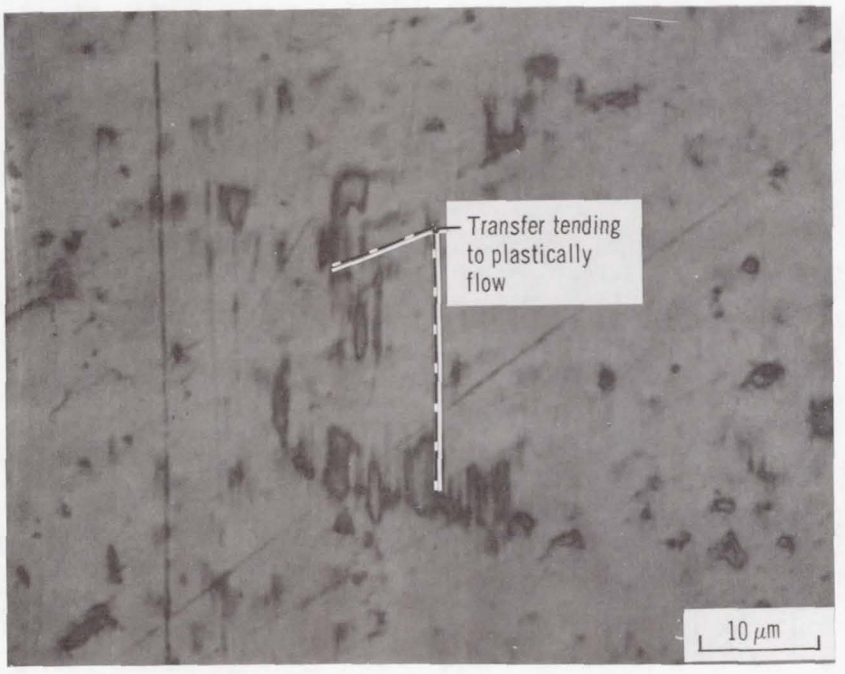

(b) Transfer from 4-BDAF/50 BTDA:50 PMDA polyimide rider.

Figure 20. - Photomicrographs of the transfer to 440C HT stainless steel disks from 4-BDAF/BTDA and 4-BDAF/50 BTDA:50 PMDA polyimide riders after 1 kilometer of sliding at 25° C and 100 rpm.

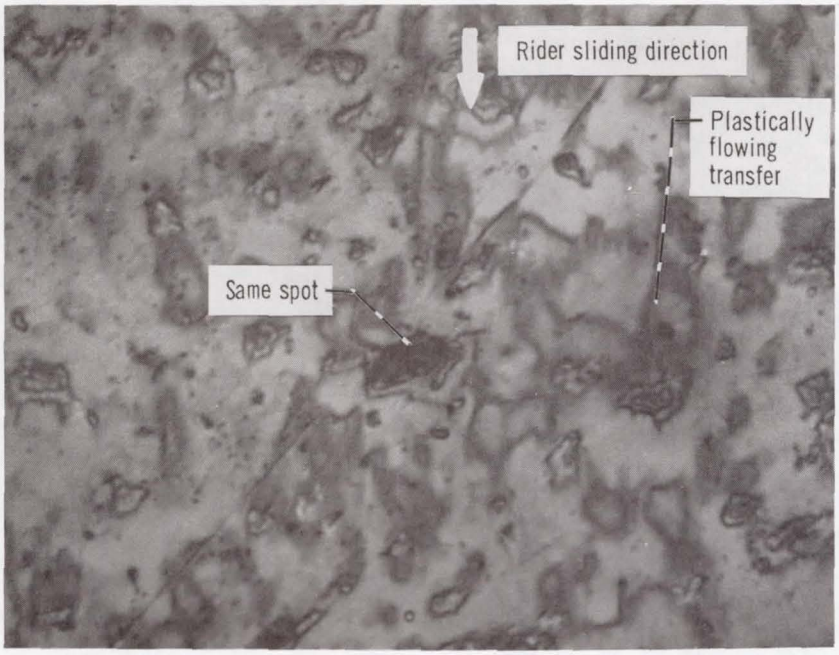

(a) 1 kilometer of sliding.

(b) 4 kilometer of sliding.

Figure 21. - Photomicrographs of the transfer to a 440C HT stainless steel disk from a 4-BDAF/BTDA polyimide composite filled with 20 weight percent PTFE after (a) 1 kilometer and (b) 4 kilometer of sliding at 25° C and 100 rpm.

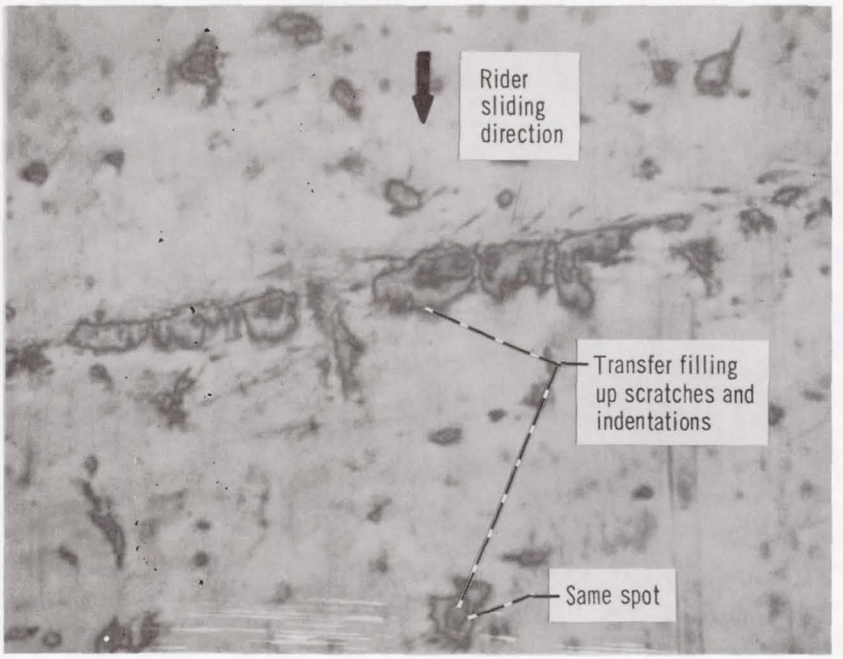

(a) 1 kilometer of sliding.

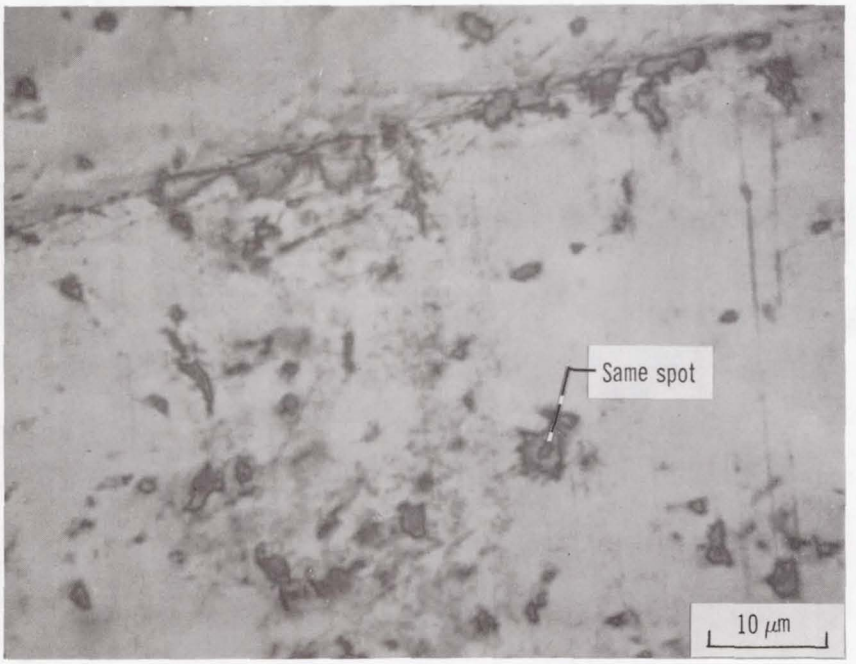

(b) 2 kilometer of sliding.

Figure 22. - Photomicrographs of the transfer to a 440C HT stainless steel disk from a non-graphtic carbon fiber (type "HC") reinforced polyimide (4-BDAF/ BTDA) composite after various sliding intervals at 25° C and 100 rpm.

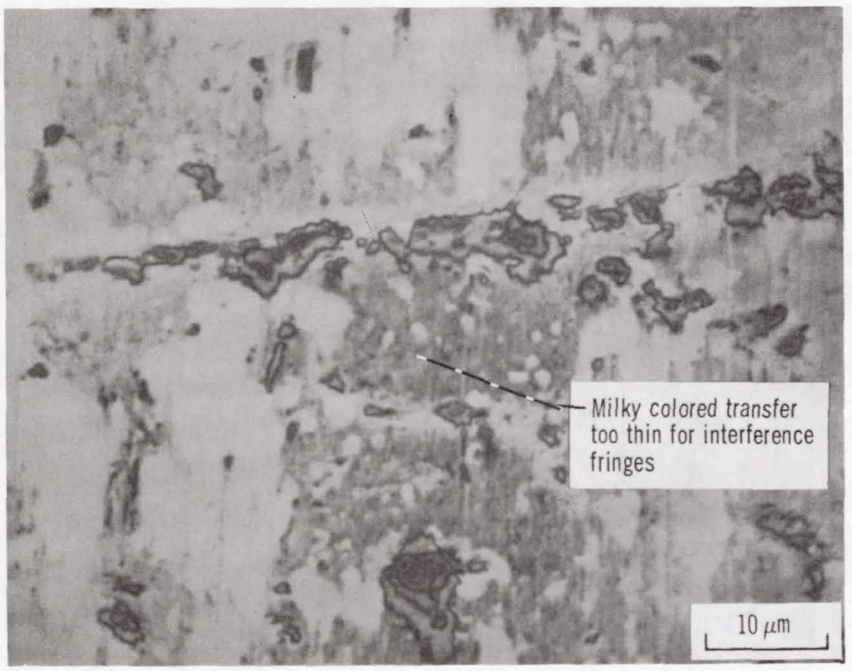

(c) 4 kilometer of sliding.

Figure 22. - Concluded

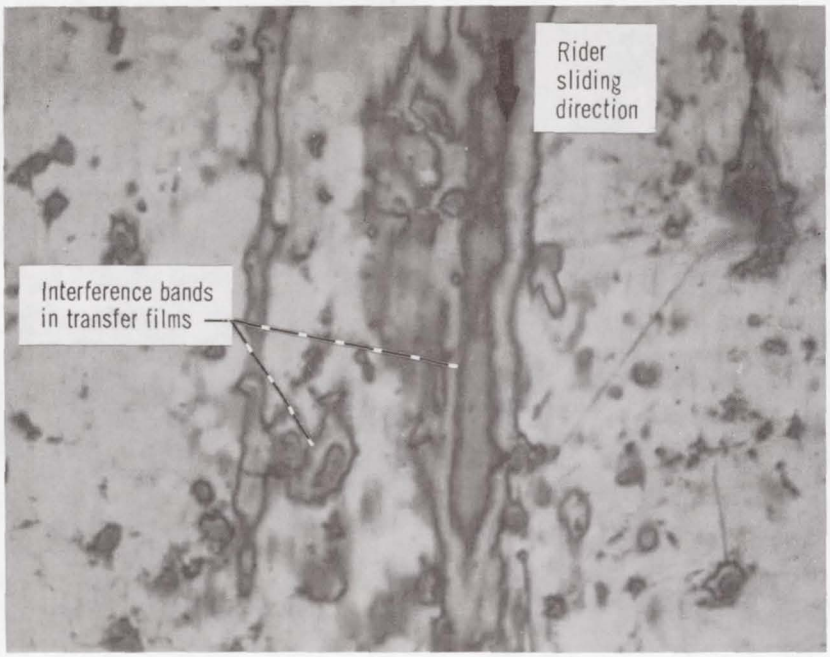

(a) 1 kilometer of sliding.

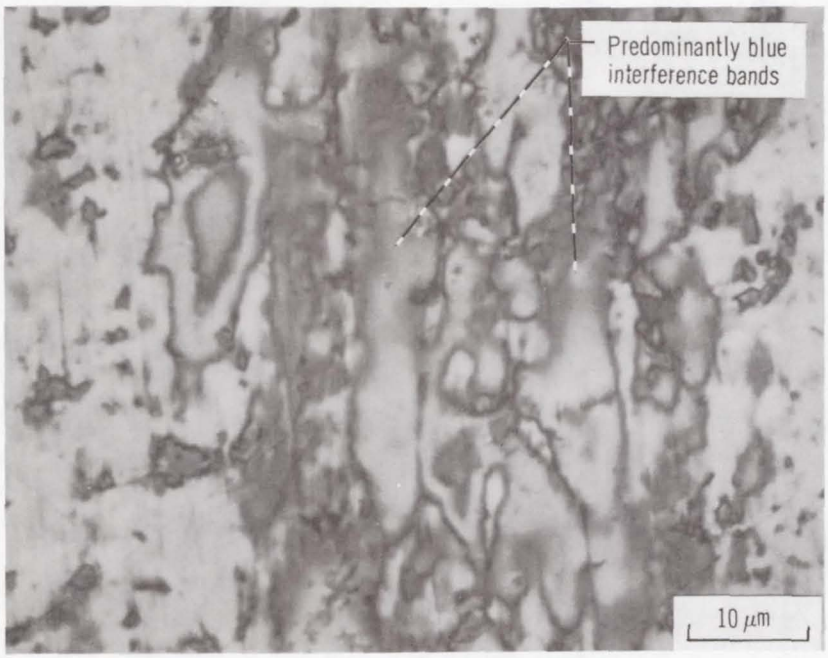

(b) 10 kilometer of sliding.

Figure 23. - Photomicrographs of the transfer to 440C HT stainless steel disks from a graphtic carbon fiber (type "HC") reinforced polyimide (4-BDAF/BTDA) composite after sliding distances of 1, 10, and 60 kilometers at 25° C and 100 rpm.

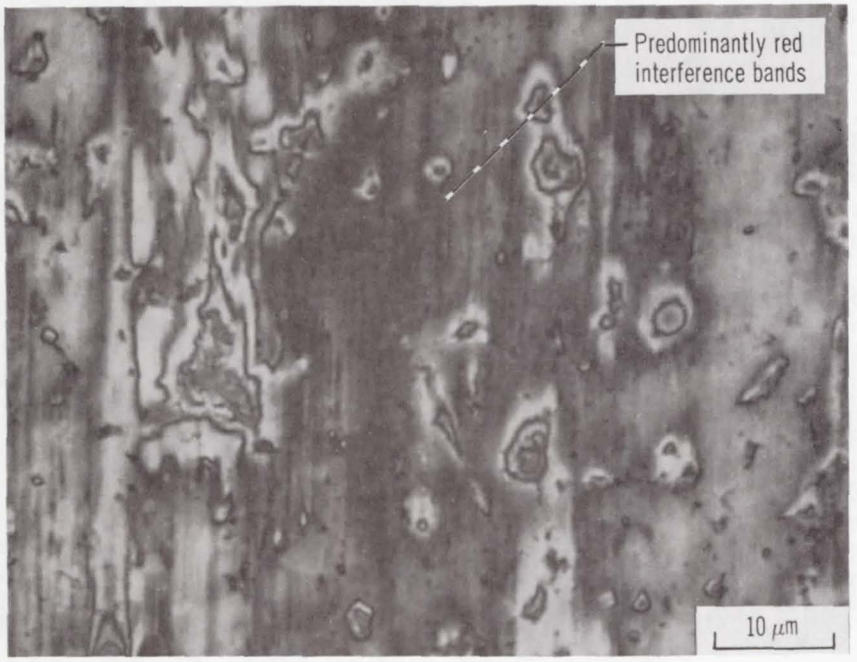

(c) 60 kilometer of sliding.

Figure 23. - Concluded.

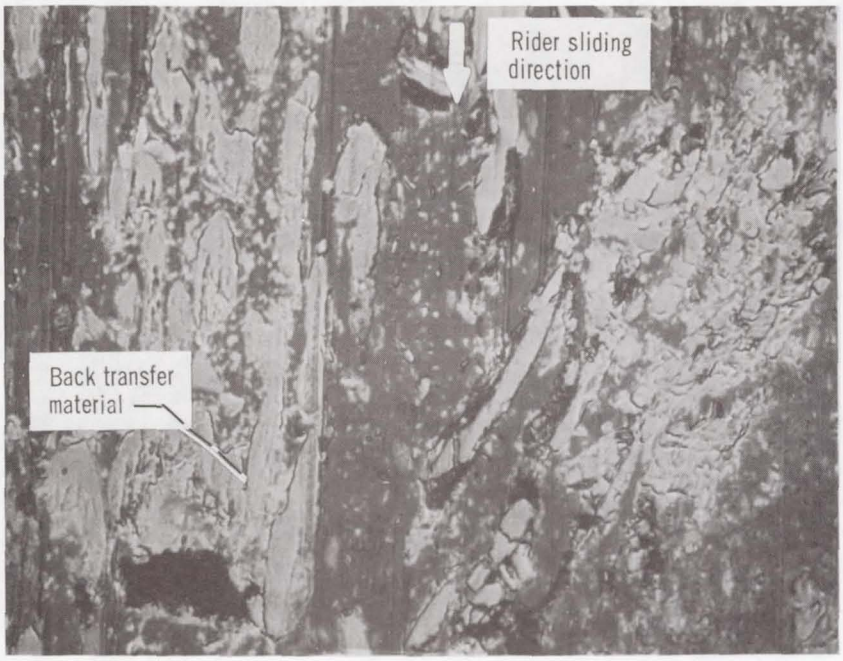

(a) 100° C.

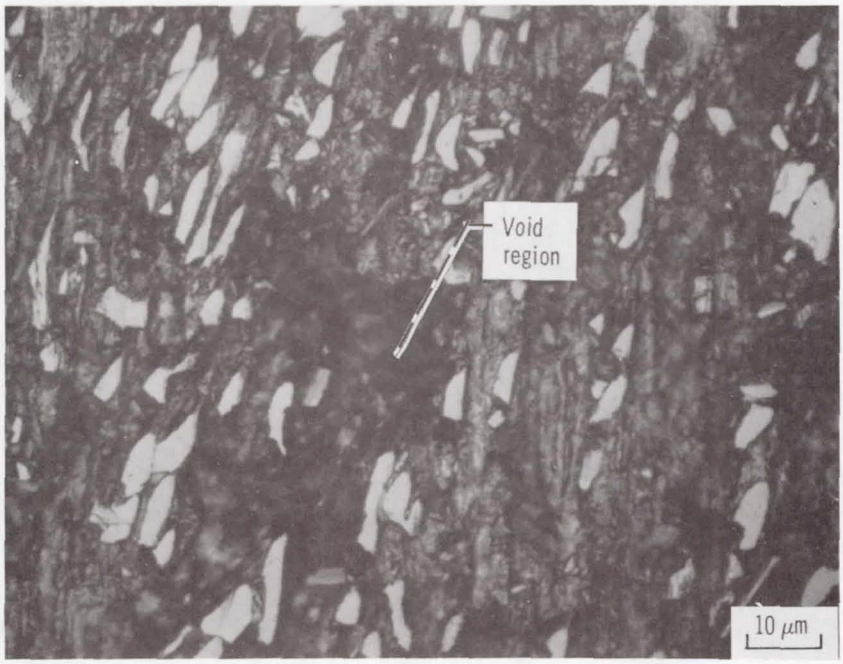

(b) 200° C.

Figure 24. - Photomicrographs of the graphitic carbon fiber (type "HG") reinforced polyimide (4-BDAF/BTDA) composite wear surface after 1 kilometer of sliding at temperatures of 100, 200, and 300° C.

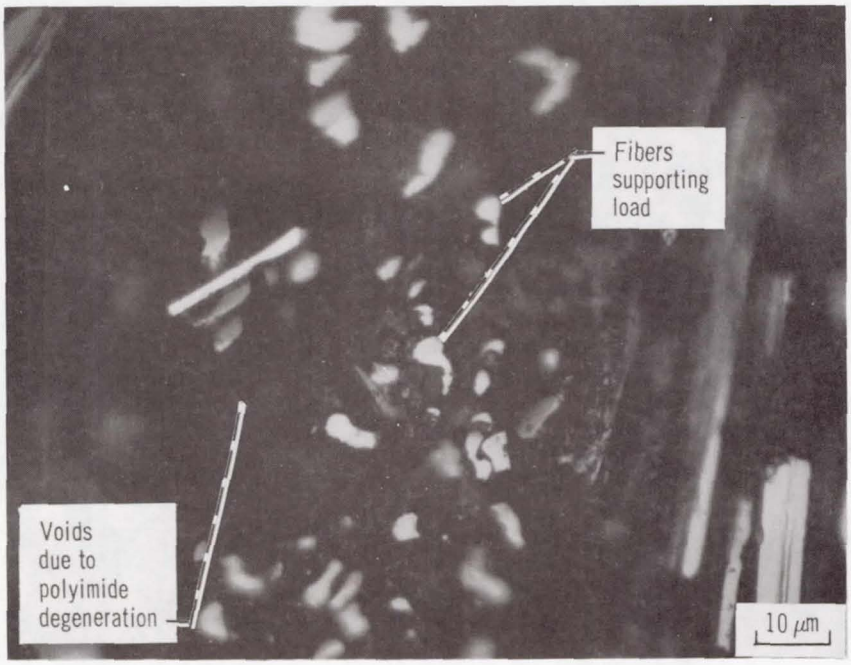

(c) 300° C.

Figure 24. - Concluded.

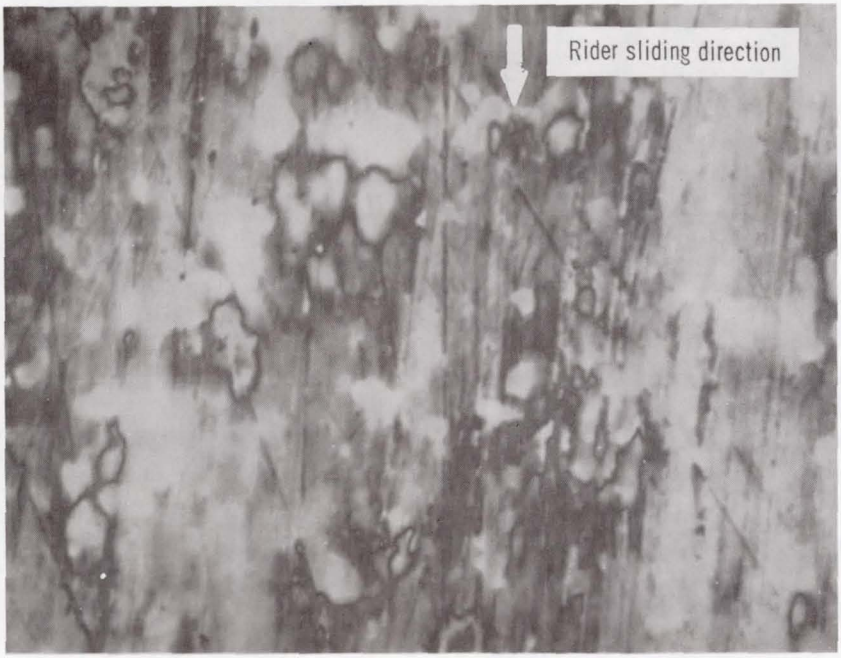

(a) 100° C.

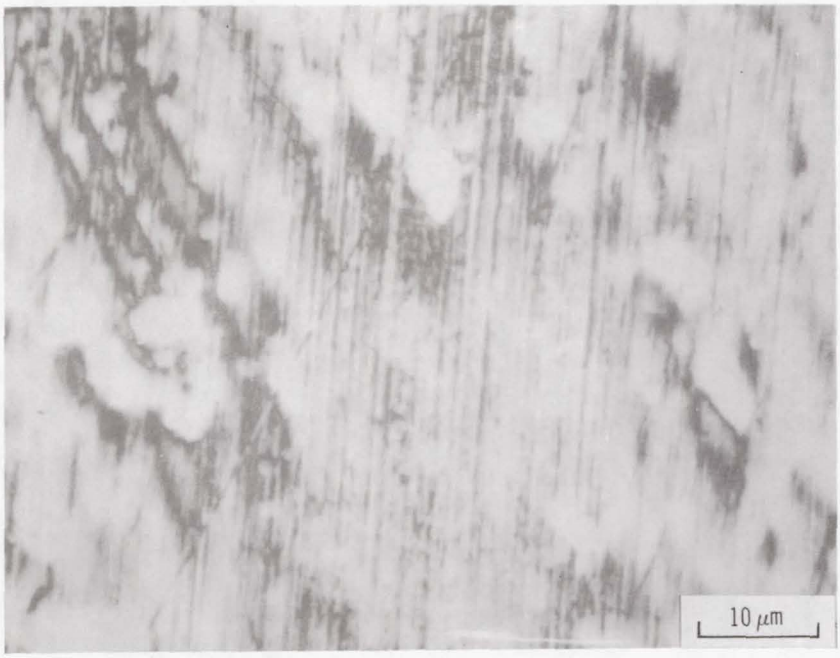

(b) 200° C.

Figure 25. - Photomicrographs of the transfer to 440C HT stainless steel disks from a graphitic carbon fiber (type "HG") reinforced polyimide (4-BDAF/BTDA) composite after 1 kilometer of sliding at temperatures of 100, 200 and 300° C.

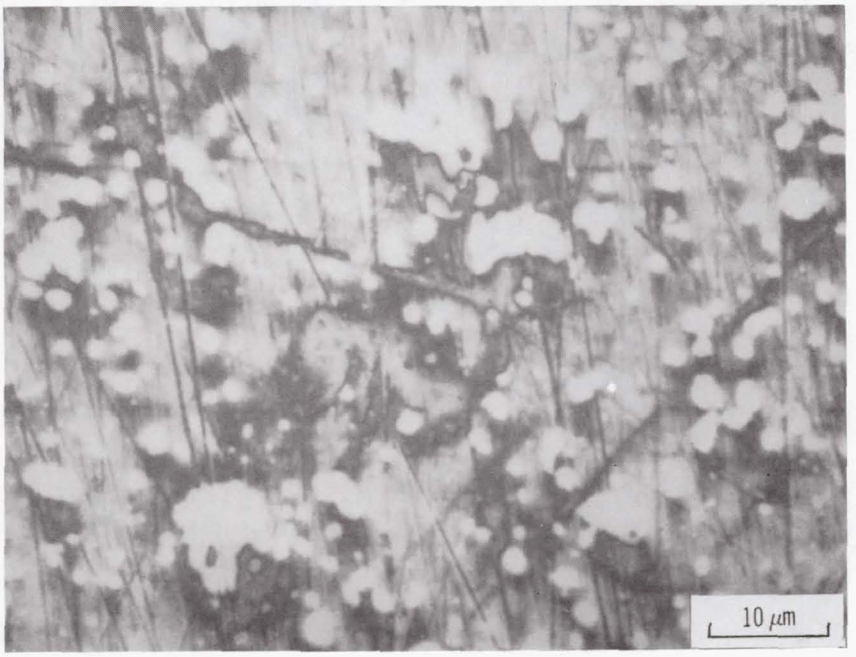

(c) 300° C.

Figure 25. - Concluded.